

## Nanoscale modification of electrical and magnetic properties of Fe<sub>3</sub>O<sub>4</sub> thin film by atomic force microscopy lithography

Motoyuki Hirooka

*Institute of Scientific and Industrial Research, Osaka University, 8-1 Mihogaoka, Ibaraki, Osaka 567-0047, Japan*

Hidekazu Tanaka

*Institute of Scientific and Industrial Research, Osaka University, 8-1 Mihogaoka, Ibaraki, Osaka 567-0047, Japan PRESTO, Japan Science and Technology Agency, Japan*

Runwei Li and Tomoji Kawai<sup>a)</sup>

*Institute of Scientific and Industrial Research, Osaka University, 8-1 Mihogaoka, Ibaraki, Osaka 567-0047, Japan*

(Received 12 December 2003; accepted 1 July 2004)

We present a report on the nanopatterning of an epitaxial ultrathin film of Fe<sub>3</sub>O<sub>4</sub> with room-temperature (ferri)magnetism using atomic force microscopy (AFM). Fe<sub>3</sub>O<sub>4</sub> thin films with atomically flat surfaces were grown using laser molecular-beam epitaxy on a MgAl<sub>2</sub>O<sub>4</sub>(111) single-crystal substrate. (Nanowire) were constructed on Fe<sub>3</sub>O<sub>4</sub> thin film by applying an electric field between an AFM conductive tip and the surface of the film. The minimum width and height in the resulting nanowire are 48 nm and 2 nm, respectively. The patterned region of the Fe<sub>3</sub>O<sub>4</sub> film surface possesses a resistance which is 10<sup>5</sup> times higher than the unpatterned region. Furthermore, magnetic force microscopy measurements also revealed that magnetization of the patterned region is strongly suppressed. © 2004 American Institute of Physics. [DOI: 10.1063/1.1784884]

Ferrimagnetic magnetite with an inverse spinel structure (Fe<sub>3</sub>O<sub>4</sub>) is one of the most abundant and important materials in the field of transition metal oxides. Fe<sub>3</sub>O<sub>4</sub> exhibits relatively high conductivity (250 Ω<sup>-1</sup> cm<sup>-1</sup>) in oxides, and possesses a half-metallic spin structure with the highest Curie temperature (850 K).<sup>1</sup> As a consequence, the construction of a spintronics device utilizing this perfect spin-polarized electron is conceivable, such as a spin tunneling magnetoresistance (TMR) and ballistic magnet-resistance (BMR) device with a high efficiency even at room temperature.<sup>2,3</sup>

The fabrication of nanostructures down to several tens of nanometers in width is indispensable for the realization of spin devices, such as the ferromagnetic single electron transistor. Nevertheless, direct modification at the nanometer scale has not been reported for magnetite.

Lithography using scanning probe microscopy (SPM),<sup>4</sup> which includes scanning tunneling microscopy (STM) and atomic force microscopy (AFM), has the potential for application in studies involving nanolithography, even with transition metal oxides. This lithography technique does not need a resist. Furthermore, the surface could be patterned down to a width of a few nanometers using a carbon nanotube as the SPM probe.<sup>5</sup>

SPM lithography has been applied to metals (Ti,<sup>6</sup> Al, and Ni<sup>7</sup>) and semiconductors (silicon,<sup>8,9</sup> Si/SiGe, and InAs/AlSb heterostructure) utilizing the electrochemical oxidation of a surface in an electrochemical cell formed by a water meniscus that develops between an AFM tip and sample surface.<sup>6,7,10</sup> There are only a few reported applications of SPM lithography to transition metal oxides, such as YBa<sub>2</sub>Cu<sub>3</sub>O<sub>7</sub>,<sup>11</sup> oxygen deficient SrTiO<sub>3</sub>,<sup>12</sup> and LiMn<sub>2</sub>O<sub>4</sub>.<sup>13</sup>

In this letter we investigate nanopatterning on a magnetite ultrathin film using atomic force microscopy, and report modifications of its electrical and magnetic properties.

The Fe<sub>3</sub>O<sub>4</sub> thin films were deposited on spinel MgAl<sub>2</sub>O<sub>4</sub>(111) single-crystal substrates using laser molecular-beam epitaxy<sup>14</sup> (ArF excimer:λ=193 nm) at a substrate temperature of 320 °C in O<sub>2</sub> at a pressure of 1.0 × 10<sup>-6</sup> mbar. The target employed was a sintered Fe<sub>3</sub>O<sub>4</sub> pellet (99.9%). Crystal structure was determined by x-ray diffraction (XRD). It was confirmed that the magnetite films grew epitaxially along ⟨111⟩ direction [*d*(111)=4.84 Å] on spinel substrates. Figure 1(a) shows an AFM image of the Fe<sub>3</sub>O<sub>4</sub> film surface (with a film thickness of 25 nm). Figure 1(b) shows vertical profile of the film. Surface roughness (rms) is 0.08 nm and an atomically flat terrace structure is clearly observed with step heights of 0.23 and 0.40 nm that correspond to the one and two atomic layers, respectively. Figure 1(c) shows the magnetic field dependence of magnetization at a temperature of 300 K, as measured by a superconducting quantum interference device (SQUID) magnetometer. This indicates that a magnetite thin film with a thickness of 25 nm shows good ferromagnetic properties at room temperature. AFM lithography was conducted on magnetite thin films utilizing a platinum coated conductive tip that scanned the surface under a biased voltage between the tip and sample surface. The sample was grounded. The tip was operated in contact mode with the lithography of the surface under an applied load of almost 0 N in air. The *I*-*V* characteristics of nanostructures formed by AFM lithography were measured using source-measure unit (Keithley) connected to the AFM tip and sample electrode. Changes in magnetization were measured by magnetic force microscopy (MFM).<sup>15</sup>

Figure 2(a) shows an AFM image of a typical nanopattern constructed on a magnetite thin film using AFM lithog-

<sup>a)</sup> Author to whom correspondence should be addressed; electronic mail: kawai@sanken.osaka-u.as.jp

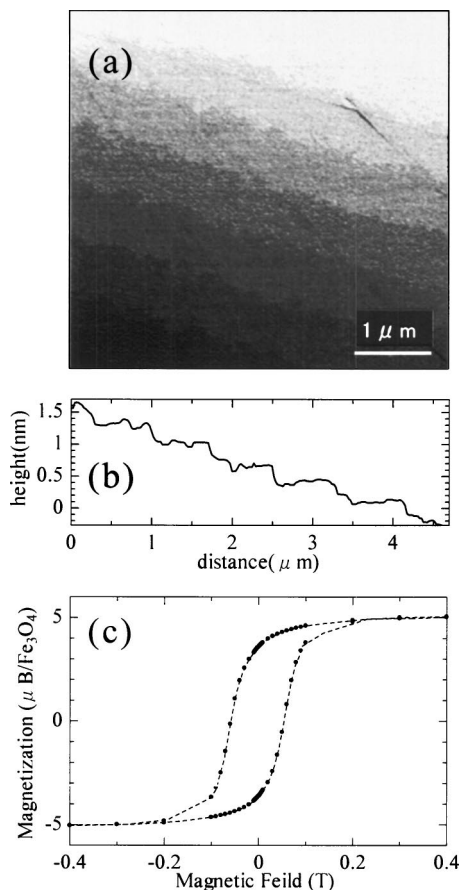


FIG. 1. (a) AFM image of the atomically flat epitaxial  $\text{Fe}_3\text{O}_4$  thin film (25 nm) on a  $\text{MgAl}_2\text{O}_4(111)$  substrate; (b) vertical profile of the sample surface; (c) magnetic field dependence of magnetization at 300 K.

raphy. The nanowire pattern was constructed using a tip voltage of  $-7$  V and a tip velocity of  $1.0 \mu\text{m/s}$ . Figure 2(b) shows the height and width of nanowires as a function of applied voltage. The voltage applied to AFM tip changes from  $-1$  to  $-10$  V at tip velocity of  $1.0 \mu\text{m/s}$ . The volume of nanowires increased (height: from 2 to 19 nm; width: from 48 to 130 nm) as the voltage increased from  $-4$  to  $-10$  V. These results confirm that the AFM lithography technique allows the electrochemical construction of nanostructures on magnetite thin films (minimum width was about 48 nm) at the nanoscale level.

Figure 3 shows the current–voltage characteristics in patterned and unpatterned region by AFM lithography. As shown in the inset of the figure, a gold electrode with a thickness of 8 nm was deposited on magnetite and a nanowire was patterned by AFM lithography from edge of gold electrode. By contacting the conductive AFM tip at point A (unpatterned region) and point B (patterned region) with a constant force of  $2.8 \times 10^{-8}$  N, the magnitude of the current was measured within the applied voltage range of  $-3$  and 3 V. Measurements of current in the patterned and unpatterned regions utilizing a tip voltage of 3 V were  $4.6 \times 10^{-10}$  and  $2.3 \times 10^{-5}$  A, respectively. In this case, the current at point (B) follows through the patterned area between tip and conducting part of film due to high resistance of the patterned area, whereas that at point (A) follows through the conducting part of film between tip and Au electrode. It is suggested that the patterned region was transformed into an insulating barrier. As electrical properties are closely con-

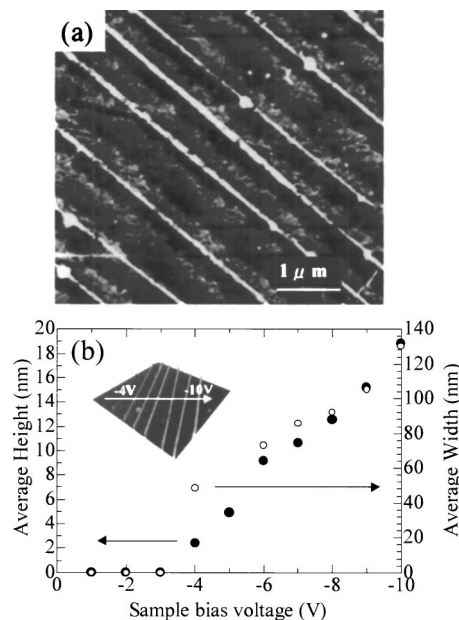


FIG. 2. (a) AFM image of nanolines written on terraces of the surface of the epitaxial  $\text{Fe}_3\text{O}_4$  thin film by AFM lithography in air ( $V_{\text{tip}}=-7$  V and scan speed  $1.0 \mu\text{m/s}$ ); (b) sample bias dependence of average height (solid circles) and average width (open circles) of nanolines fabricated by AFM lithography. The inset shows a 3D image of the surface after nanopatterning at a tip bias of  $-4, -5, -6, -7, -8, -9,$  and  $-10$  V, respectively.

nected to magnetism in transition metal oxides, it is expected that the magnetism of patterned region would also be modified by AFM lithography. Changes of the magnetic properties of the nanopatterned region were observed using MFM with a cobalt-coated silicon tip. Figure 4(a) shows a MFM image measured by phase detection. Magnetic domain structures with a width of  $0.15 \mu\text{m}$  appear in the unpatterned film surface, but magnetic domain structures are not present in the patterned region. Figure 4(b) shows the cross-sectional profile of a MFM image. Remarkably, the phase shift in the patterned region almost became zero. Moreover, the phase shift contrast in the patterned region appears almost monotonically without any magnetic poles especially in the both edges of in the patterned region, indicating no magnetic field was detected. We suggest that magnetization is decreased in the patterned region as a result of AFM lithography.

Basically, AFM lithography creates an electrochemical reaction by scanning a biased probe close to the experimental surface.<sup>5,8</sup> Via ambient humidity, a water meniscus is formed between the probe and the surface. An electrochemical cell is formed, and sample surface is oxidized to produce a variety

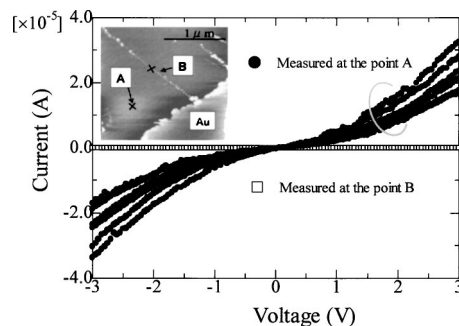


FIG. 3.  $I$ - $V$  curves measured at point A (unpatterned area) and point B (patterned area).

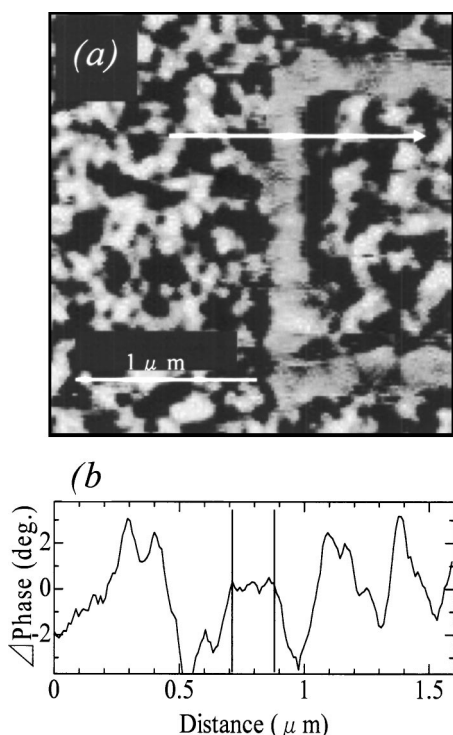


FIG. 4. MFM image of a  $\text{Fe}_3\text{O}_4$  surface patterned by AFM lithography with a  $-6$  V tip bias in air, and vertical profile.

of well-known oxides, such as  $\text{Fe}_3\text{O}_4$ ,<sup>22,23</sup>  $\gamma\text{-Fe}_2\text{O}_3$ ,<sup>20,21</sup>  $\alpha\text{-Fe}_2\text{O}_3$ ,<sup>18,19</sup> and  $\text{FeO}$ <sup>17</sup> (Table I). If electrochemical oxidation occurs by AFM lithography on  $\text{Fe}_3\text{O}_4$  thin films like metals and semiconductors, it seems that  $\text{Fe}_3\text{O}_4$  is simply oxidized into  $\alpha\text{-Fe}_2\text{O}_3$ , if considering the oxidation reaction of  $\text{Fe}^{2+} \rightarrow \text{Fe}^{3+}$ , which results in the oxide behaving like an antiferromagnetic insulator. The experimental results relating to insulating electrical properties and deduced (suppressed) magnetism in the patterned region agree with the physical properties of  $\alpha\text{-Fe}_2\text{O}_3$ . Because  $\gamma\text{-Fe}_2\text{O}_3$  exhibits ferrimagnetism with a similar degree of magnetization, the possibility

TABLE I. Electrical and magnetic properties of iron-based oxides. ( $T_N$ ,  $T_C$ ),  $\rho_{(300\text{ K})}$ , and  $M_{(300\text{ K})}$  are Néel (Curie) temperature, resistivity, and magnetization at 300 K, respectively. Data are taken from Refs. 17–23.

Material	Valence	Electrical property	Magnetism
FeO	2+	insulator	antiferromagnetic ( $T_N=198$ K)
		semimetal	ferrimagnetic ( $T_C=850$ K,
$\text{Fe}_3\text{O}_4$	2.5+ (mixed valence)	$\rho_{(300\text{ K})}$ $=4.0 \times 10^{-3} \Omega \text{ cm}$	$M_{(300\text{ K})}=90$ emu/g) antiferromagnetic ( $T_C=948$ K,
$\gamma\text{-Fe}_2\text{O}_3$	3+	(insulator)	$M_{(300\text{ K})}=65$ emu/g) ferrimagnetic ( $T_C=958$ K,
$\alpha\text{-Fe}_2\text{O}_3$	3+	insulator	$M_{(300\text{ K})}=0.4$ emu/g)

of the presence of  $\gamma\text{-Fe}_2\text{O}_3$  can be ruled out. Additionally, as  $\text{FeO}$  is an antiferromagnetic insulator that is formed by reduction from  $\text{Fe}_3\text{O}_4$  ( $\text{Fe}^{3+} \rightarrow \text{Fe}^{2+}$ ), the possibility of its presence can also be ruled out. From the standpoint of electrochemical oxidation,  $\alpha\text{-Fe}_2\text{O}_3$  is a possible candidate as the material present in the patterned region. However, it would not explain the large expansion of volume of the patterned region. An amorphous or poorly dense  $\alpha\text{-Fe}_2\text{O}_3$  is the most likely candidate as the component of the patterned region because the high voltage was applied to the local area. Additional research has revealed that the patterned region of  $\text{Fe}_3\text{O}_4$  can be selectively etched by HCl solution and completely removed (unpublished data), as already reported for  $\text{SrTiO}_{3-\delta}$ .<sup>16</sup>

In conclusion, we fabricated  $\text{Fe}_3\text{O}_4$  epitaxial thin films with atomically flat surfaces using laser molecular-beam epitaxy, and used such surfaces to conduct AFM lithography experiments. The application of a negative voltage to the AFM cantilever tip systematically formed nanowires, even with the ferrimagnetic oxide of  $\text{Fe}_3\text{O}_4$ . The physical properties of the nanopatterned area were changed to resistive state that was  $10^5$  times higher in the electrical conductivity, and a resulting magnetization state that approached zero magnetism. Indeed, the application of this technique to high  $T_C$  ferromagnetic oxides opens the possibility for the construction and development of nanoscale spintronics devices.

<sup>1</sup>Z. Zhang and S. Satpathy, Phys. Rev. B **44**, 13319 (1991).

<sup>2</sup>X. W. Li, A. Gupta, G. Xiao, W. Qian, and V. P. Dravid, Appl. Phys. Lett. **73**, 3282 (1998).

<sup>3</sup>J. J. Versluijs, M. A. Bari, and J. M. D. Coey, Phys. Rev. Lett. **87**, 026601 (2001).

<sup>4</sup>R. M. Nyffenegger and R. M. Penner, Chem. Rev. (Washington, D.C.) **97**, 1195 (1997).

<sup>5</sup>H. Dai and N. Franklin, Appl. Phys. Lett. **73**, 1508 (1998).

<sup>6</sup>H. Sugiyama, T. Uchida, N. Kitamura, and H. Masuhara, Jpn. J. Appl. Phys., Part 2 **32**, L553 (1993).

<sup>7</sup>Y. Takemura, S. Kidaka, K. Watanabe, Y. Nasu, and T. Yamada, J. Appl. Phys. **93**, 7346 (2003).

<sup>8</sup>A. E. Gordon, R. T. Fayfield, D. D. Litfin, and T. K. Higman, J. Vac. Sci. Technol. B **13**, 2805 (1995).

<sup>9</sup>J. A. Dagata, J. Schneir, H. H. Harary, C. J. Evans, M. T. Postek, and J. Bennett, Appl. Phys. Lett. **56**, 2001 (1990).

<sup>10</sup>Z. H. Chen, S. W. Huang, and J. G. Hwu, Solid-State Electron. (2003).

<sup>11</sup>R. E. Thomson, J. Moreland, and A. Roshko, Nanotechnology **5**, 57 (1994).

<sup>12</sup>L. Pellegrino, I. Pallecchi, D. Marre, E. Bellingeri, and A. S. Siri, Appl. Phys. Lett. **81**, 3849 (2002).

<sup>13</sup>R. Kostecki and F. McLarnon, Appl. Phys. Lett. **76**, 2535 (2000).

<sup>14</sup>H. Yahihiro, H. Tanaka, Y. Yamamoto, and T. Kawai, Solid State Commun. **123**, 535 (2002).

<sup>15</sup>D. W. Abraham and F. A. McDonald, Appl. Phys. Lett. **56**, 1181 (1990).

<sup>16</sup>E. Bellingeri, L. Pellegrino, I. Pallecchi, A. S. Siri, and D. Marre, Solid-State Electron. **47**, 2193 (2003).

<sup>17</sup>W. L. Roth, Phys. Rev. **110**, 1333 (1958).

<sup>18</sup>P. J. Flanders and W. J. Schuele, Philos. Mag. **9**, 485 (1964).

<sup>19</sup>P. J. Flanders, Philos. Mag. **11**, 1271 (1965).

<sup>20</sup>G. A. Ferguson, Jr. and M. Hass, Phys. Rev. **112**, 1130 (1958).

<sup>21</sup>Y. Goto, Jpn. J. Appl. Phys. **3**, 739 (1964).

<sup>22</sup>G. A. Samara, Phys. Rev. **186**, 577 (1969).

<sup>23</sup>B. A. Calhoun, Phys. Rev. **94**, 1577 (1954).